Flow Forming of Wood Irradiated with Electron Beam — Molding Load of Irradiated Wood and Mechanical Properties of the Molded Material

Hideaki Sugino,[a] Soichi Tanaka,[b,*] Yuga Kasamatsu,[c] Satoko Okubayashi,[b,d] Masako Seki,[e] Tsunehisa Miki,[e] Kenji Umemura,[b] and Kozo Kanayama [b]

In the flow forming technique of wood, a wood block is flowed into metal dies to mold the material into a three-dimensional complex shape. The purpose of this study was to investigate the effect of molding load and the mechanical properties of the molded material in the case that wood as a raw material was irradiated with electron beam (EB). The EB-irradiated wood board was impregnated with thermosetting resin and was subsequently molded into the material by adding pressure and heating in a closed metal die. It was found that the molding load of the impregnated wood was decreased with increasing the EB absorbed dose. The mechanical properties of the molded material were evaluated using modulus of elasticity (MOE) and modulus of rupture (MOR) in a three-point bending test. With increasing EB dose, MOR decreased greatly, while MOE decreased slightly. The EB irradiation on raw wood made it possible to mold the material at low load, though higher dose irradiation caused larger decreases in the mechanical properties.

Keywords: Electron beam irradiation; Wood flow forming; Molding load; Mechanical properties

*Contact information: a: GISEN Co., Ltd., 501-0234, Japan; b: Research Institute for Sustainable Humanosphere, Kyoto University, 611-0011, Japan; c: Meisei Chemical Works Ltd., 615-8666, Japan; d: Department of Advanced Fibro- Science, Kyoto Institute of Technology, 606-8585, Japan; e: Multi-Material Research Institute, National Institute of Advanced Science and Technology, 463-8560, Japan; * Corresponding author: mailto:soichi_tanaka@rish.kyoto-u.ac.jp*

INTRODUCTION

Wood flow forming is a new technique in wood processing (Yamashita *et al.* 2007; Seki *et al.* 2017). In this technique (Fig. 1), one or several wood blocks are flowed into the metal dies to mold a material with three-dimensional complex shape. The molding process includes the heating, pressing, and cooling in the mold. In this process (Miki *et al.* 2014), each wood structure (Fig. 1a) is separated near the intercellular layer into smaller parts (Fig. 1b), and the material is subsequently flowed into the empty space in the mold. The separated parts are re-bonded to each other (Fig. 1c) and then fixed. In the molding process, wood fibers are protected from rupture, and thus the mechanical properties of the molded material are higher than other molded compact structures made of wood powders and mechanical pulps.

The molding load is one of the important factors for the industrial application of the wood flow forming. The molding load is mainly affected by the flow deformation of wood. For the easier flow deformation, the pre-treatment to soften the intercellular layers is effective. Pre-treatments such as additive impregnation (Miki *et al.* 2015), moisture control (Miki *et al.* 2014), and chemical modification (Seki *et al.* 2016a) have been

investigated. To promote the industrial application more widely, the molding load is required to be further decreased. For the further decrease in the molding load, it is necessary to consider an active treatment that partially decomposes or dissolves wood. A chemical treatment such as an alkaline treatment can be classed as an active treatment. However, it generally requires a complicated process that leaves residual chemicals after the treatment (Saito *et al.* 2016). Thus, a physical treatment is desirable as the pre-treatment for the wood flow forming.

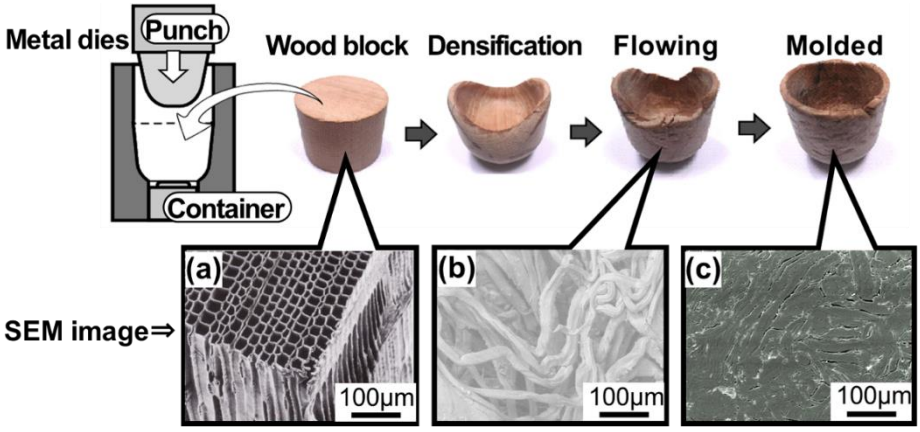

Fig. 1. Wood flow forming technique and fiber structure in each process (Tanaka 2017)

Electron beam (EB) irradiation is the physical treatment considered in this study. The EB is a type of ionizing radiation, and it has some advantages when it is compared to other ionizing radiations such as gamma rays and ultraviolet light (Kashiwagi and Hoshi 2012). For example, the EB is easily manipulated because it is electrically controlled without any radioactive elements. In another example, the EB penetrates wood more easily than UV light. Thus, the EB irradiation has been widely used in industry (Mehnert 1996; Kashiwagi and Hoshi 2012).

The influence of the EB irradiation on the polymer materials can be categorized as two types (Nakai *et al.* 2009). One is the promotion of the cross-linking of polymers and graft polymerization. Another is the cleavage of chemical bonds. To improve wood properties, the cleavage effect has especially been applied, for example, in pre-treatment for enzymolysis (Ma *et al.* 2014; Leskinen *et al.* 2017) and improvement of weatherability (Schnabel and Huber 2014). The flow deformation is expected to occur in the low molding load by EB irradiation of raw wood.

In a previous paper (Sugino *et al.* 2020), the stress for starting the flow deformation of wood was successfully decreased by the EB irradiation of raw wood. This result showed that EB irradiation may partially break chemical bonds in wood. It was also suggested that the mechanical properties of molded materials may be decreased by the EB irradiation on the raw wood. This may be the fatal problem in industrial material utilization. It is therefore necessary to investigate simultaneously the molding load of wood and the mechanical properties of the molded material.

This study investigated the mechanical properties of the molded material using EB-irradiated wood as a raw material. The EB-irradiated wood board was molded into the material in closed metal dies, and the mechanical properties of the molded material was evaluated by three-point bending tests. The relationship between the molding load and the mechanical properties is discussed.

EXPERIMENTAL

Materials

Twenty-nine pieces of flat-sawn boards (228 mm (L) × 40 mm (T) × 2 mm (R)) were continuously cut along the R direction from the rectangular block of heartwood of hinoki (*Chamaecyparis obtusa*). Fifteen pieces were selected from the boards so that the difference in density among them was as small as possible. Four oval disks (55 mm (major axis, L) × 28 mm (minor axis, T) × 2 mm (thickness axis R)) were cut from each selected piece. The oval disks were dried in a convection oven (105 °C) for 18 h and subsequently placed in a desiccator with dried silica gel.

Methods

The experimental procedures are shown in Fig. 2.

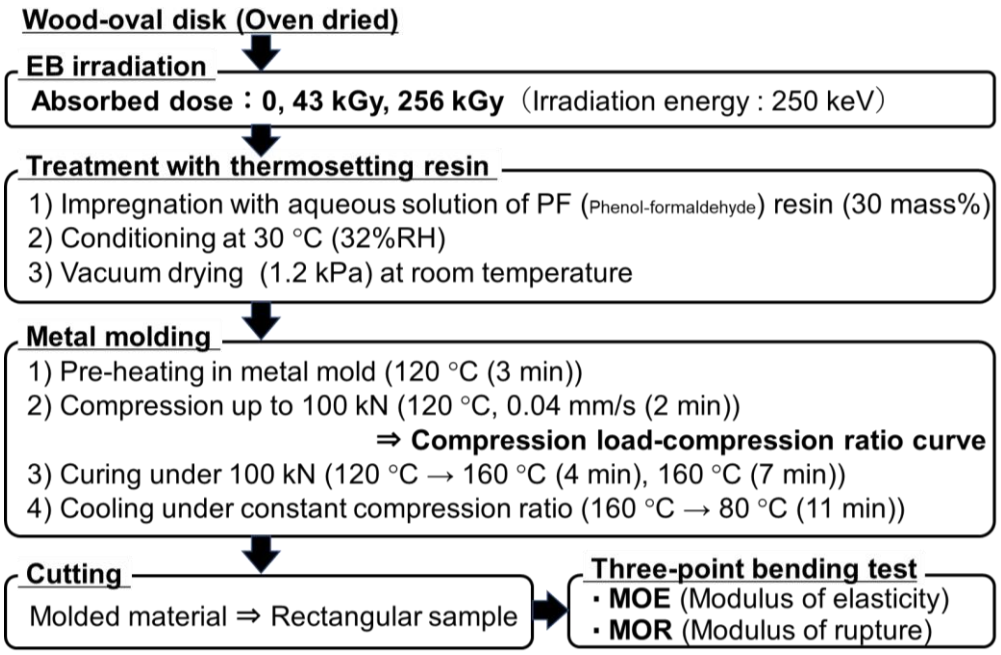

Fig. 2. Experimental procedures

EB irradiation

The oven-dried oval disks were divided into three groups according to three levels of the absorbed dose of EB. Four or five disks each in the same group were enclosed in a nylon plastic bag (Hiryu HN Type, Asahikasei Pax Co., Tokyo, Japan) with the plane shape (17 cm × 7 cm) in the air at 44% relative humidity (RH) (21 °C). The enclosed bags were placed in a closed container with the dried silica gel until the EB irradiation.

The EB was vertically irradiated on the plane surface of the disks-enclosed bags by an EB irradiation system (Curetron EBC-300, NHV Co., Kyoto, Japan) with an accelerating voltage of 300 kV. The space (73 mm distance) between the bags and the irradiation window made of titanium was fully filled with nitrogen gas, and thereby the EB energy irradiated on the bags was approximately 250 keV. In the three groups, the bags for the first and the second groups were irradiated with EB one time and six times, respectively, from each two wider surfaces. The bags for the third group were not irradiated at all.

The EB was also irradiated vertically on the plane surface of the piled sheets of blue cellophane with a thickness of 0.023 mm for one sheet. The absorbance was measured for each sheet to estimate the distribution of the EB absorbed dose in a wood disk, where it was assumed that the types and contents of the chemical elements for blue cellophane was the same as that for wood and the nylon plastic bag. If the EB was irradiated on the disk once from its each two wider surfaces, the absorbed dose was estimated to be distributed in the disk along the thickness-direction (52.8 kGy (maximum) on its surface plane and 28.8 kGy (minimum) on its center plane). In this case, the average dose absorbed on the disk was estimated to be 42.7 kGy. Thus, the disks for the first and the second groups were estimated to absorb EB with the dose of 43 kGy and 256 kGy, respectively, while the disks for the third group absorbed undoubtedly 0 kGy EB. The estimated dose was used as an indicator of the absorbed dose of EB for each group. This dose was close to the dose in the previous paper (Sugino *et al.* 2020).

The disks were maintained in the bag for 3.5 h after the EB irradiation, and they were subsequently taken out from the bag to be heated in a convection oven (105 °C) for 50 h. The disks without EB irradiation were also heated to experience the same thermal history as those with EB irradiation.

Treatment with thermosetting resin

Phenol-formaldehyde (PF) resin (PX-341, Aica Kogyo Co., Nagoya, Japan; original solid content is 50 mass%) was selected as the thermosetting resin. This resin is cured at 160 °C and softens the intercellular layer at 120 °C (Miki *et al.* 2012) to promote the flow deformation of wood.

The heated disks were impregnated with an aqueous solution of the PF resin with a solid content of 30 mass % in the pressure vessel. In the impregnation, the disks were vacuumed for 1 h to an absolute pressure of 0.9 kPa, subsequently soaked in the solution with maintaining the vacuumed state, and placed in the solution for 29 h at an atmospheric pressure to be impregnated. The impregnated disks were taken out of the solution, wiped with a paper towel to remove the dripping solution, and conditioned in a closed container (32% RH, 30 °C) for 66 h. The conditioned disks were dried in a vacuum for 40 h (1.2 kPa), and subsequently preserved as the treated disks in a desiccator with dried silica gel until the metal molding began.

Metal molding

The universal testing machine (5582, Instron, Norwood, MA, USA) and a set of the metal dies (container and punch) were used to mold the materials from the treated disks with an oval shape (Fig. 3). The cylindrical container with the inner and outer diameters of 55 mm and 113 mm, respectively, and the height of 60 mm was placed on the plane metal base mounted on the testing machine, and the lower punch with 55 mm diameter and 20 mm height was inserted in the container to be contact with the base. The container was wound by the band heater so that the inside was heated to 120 °C. Two treated disks were piled on the lower punch so that their fiber directions were in parallel to each other and so that the pith side of both disks were directed to the lower punch. The upper punch with 55 mm diameter and 20 mm height, being preliminarily heated to 120 °C, was inserted into the container to be put on the piled disks. The load was applied on the upper punch by the head of the testing machine through a metal rod with 53 mm-diameter and 65 mm-height. Here, the lubricant was sprayed in advance on the sliding surface between the punches and

container to reduce the friction on the surface and the flow of the resin into the space between the punches and container. Prior to the molding, the contact surface of the two punches with the disks was polished to have surface roughness of R_z = 0.4 μm and was coated with CrN by a physical vapor deposition (PVD) treatment.

The head of the testing machine moved downward at constant rate of 0.04 mm/s to compress the disks at 120 °C up to 100 kN. During the compression of the disks, the compression load P and the apparent distance between two punches h_s were measured. The compression without the disks was also performed to obtain the deformation characteristics of the metal dies, or the relation of the reference distance between two punches h_b to the compression load P. The corrected distance h (P) was calculated as $h_s(P) + h_b(P)$. The compression ratio r was defined as $1 - h/h_0$, where h_0 represents the thickness of the piled disks along the R-axis. Immediately after the disk compression, the temperature inside the container was increased from 120 °C to 160 °C for 4 min and subsequently kept at 160 °C for 7 min with the compression load maintained at 100 kN. This was performed for the curing of the resin in the disks. The container was cooled to 80 °C inside for 11 min by replacing the band heater with the cooling jigs connected to cooled water circulating apparatus. The molded material with a shape of circular disk (55 mm-diameter and 1 mm-thickness) was removed from the container. The fiber direction in the material was oriented in one direction, indicating that the wood was uniformly flowed perpendicular to fiber direction to fill up the space in the metal dies (Fig. 3).

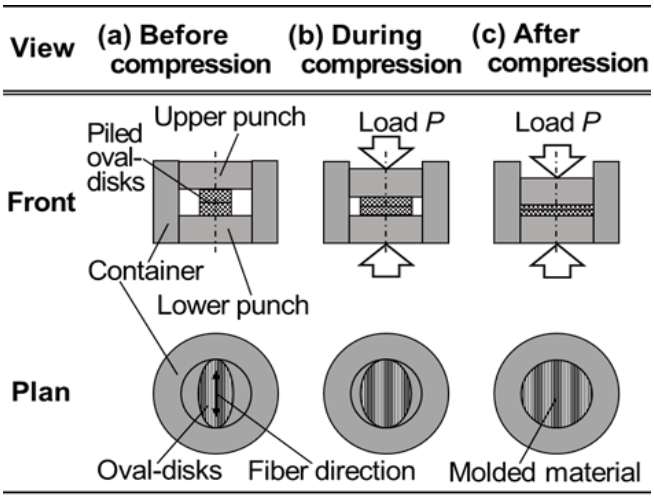

Fig. 3. Compression process in a metal molding

The densification load, the flow starting load, and the molding load were estimated using the compression load-compression ratio curve (Fig. 4). The flow starting load P_f was defined as the compression load at which the derivative of the load with respective to the compression ratio reached to the maximum value in the range of 50 to 70% compression ratio. The densification load P_d and the molding load P_m are defined in the following equations,

$$P_d = \frac{1}{r_f - r_p} \int_{r_p}^{r_f} P dr \quad (1)$$

$$P_m = \frac{1}{r_m - r_f} \int_{r_f}^{r_m} P dr \quad (2)$$

where r_p, r_f, and r_m represent the proportional limit ratio, flow starting ratio, and the maximum ratio (Fig. 4), respectively.

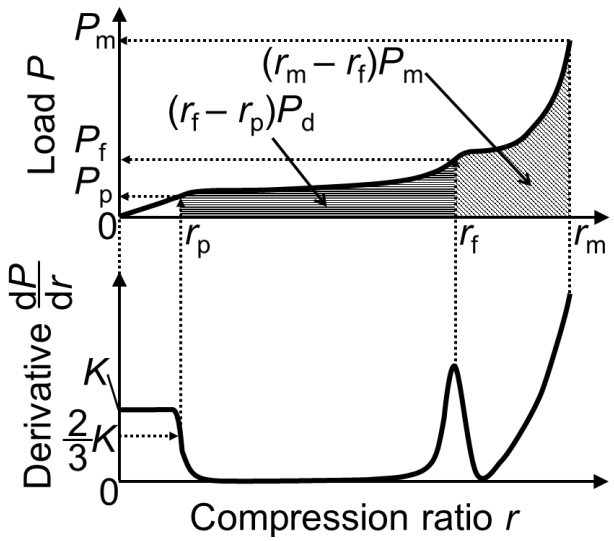

Fig. 4. Method to evaluate molding characteristics. K represents elastic coefficient in compression, r_p, r_f, and r_m are the proportional limit ratio, flow starting ratio, and the maximum ratio, P_p, P_f, and P_m are the proportional limit load, flow starting load, and the maximum load, P_d and P_m are the densification load and the molding load, respectively.

Three-point bending test

The rectangular sample with a dimension of 20 mm (L direction in the original oval disk) × 4 mm (T direction in the original oval disk) × 1 mm (R direction in the original oval disk) was cut from the molded material in the center. The cut surface was polished using lapping film (Grit 4000, 3M Company, Saint Paul, MN, USA) prior to the three-point bending test.

The three-point bending test was performed using the universal testing machine (4411, Instron) and the custom-made jig. The distance between the supporting points was 20 mm. The rectangular sample was placed on the supporting points so that its pith side before the molding was directed to the supporting points. The loading point moved toward the sample to measure the load-displacement curve at the displacement speed of 1 mm/min. The stress-strain curve was obtained from the load-displacement curve. The modulus of rupture (MOR) of the sample was estimated as the maximum value of the stress in the stress-strain curve. The modulus of elasticity (MOE) of the sample was estimated as the slope of the s-s curve in the linear region.

RESULTS AND DISCUSSION

Properties of Oval Disks before Molding Process

Table 1 shows the mass, volume, and density of each two oval disks used in one molding process. The oval disks before and after both the EB irradiation and the resin-treatment did not have so much difference in the mass, volume, and density among all the absorbed doses. This result indicates that there was little influence of the absorbed doses on the amount of both cell walls and resin included in each two disks.

Table 1. Mass, Volume, and Density of Each Two Oval Disks Used in One Molding Process (n = 5)

Absorbed Dose (kGy)	Before EB Irradiation (Oven-dried)			After Resin Treatment (Vacuum-dried)		
	Mass (g)	Volume (cm^3)	Density (g/cm^3)	Mass (g)	Volume (cm^3)	Density (g/cm^3)
0	2.36 ± 0.23	4.78 ± 0.04	0.49 ± 0.04	4.01 ± 0.05	5.34 ± 0.03	0.75 ± 0.01
43	2.24 ± 0.06	4.77 ± 0.04	0.47 ± 0.01	3.99 ± 0.06	5.38 ± 0.14	0.74 ± 0.02
256	2.25 ± 0.06	4.75 ± 0.05	0.47 ± 0.01	3.87 ± 0.07	5.21 ± 0.06	0.74 ± 0.01

Flow deformation behavior of wood in molding process

The representative compression load-compression ratio (*l*-*r*) curve is shown in Fig. 5 for each absorbed dose. The compression load over all range of the compression ratio tended to decrease with increasing absorbed dose. The compression load especially in the range of 50 to 80% compression ratio was greatly affected by the absorbed dose.

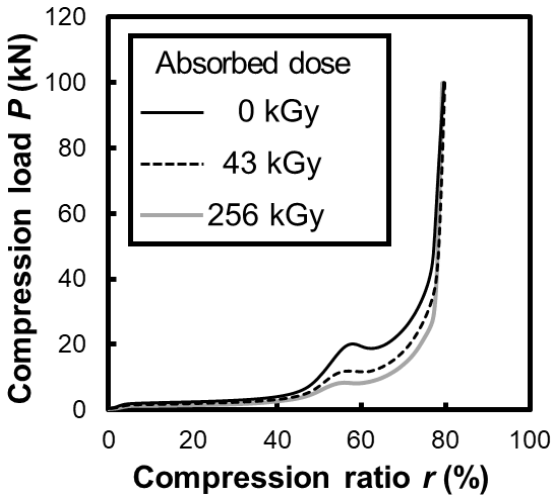

Fig. 5. Representative load-compression ratio curves during molding for each absorbed dose

Figure 6 shows the flow starting ratio and the maximum ratio estimated from the *l*-*r* curve. The maximum ratio, indicating the compression ratio at which the compression load reached to 100 kN, was not affected by the absorbed dose. This result is explained by two factors. The first factor was little influence of the absorbed dose on the amount of both cell walls and resin included in each two disks (Table 1). The second factor was that the space in the closed metal dies was always fulfilled by the flowed disks irrespective of the dose. The flow starting ratio (Fig. 6), indicating the compression ratio at which the disks started to flow, also was not affected by the absorbed dose. This suggests that the flow deformation did not start until almost all the cell cavities were compressed in the densification deformation.

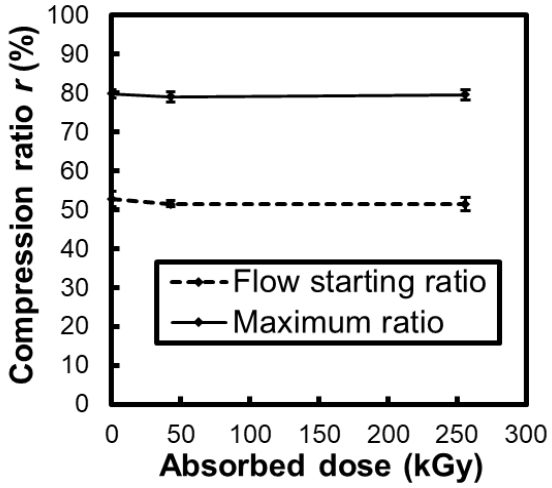

Fig. 6. Relation of flow starting and maximum ratios to absorbed dose. Error bars represent standard deviations (n = 5).

Compression load required to each deformation

Figure 7 shows the densification load, the flow starting load, and the molding load estimated from the *l*-*r* curve (Fig. 5). The densification load was almost constant for all absorbed doses, and the flow starting load decreased with increasing dose. This tendency is consistent with the result when only water was impregnated before the flow deformation (Sugino *et al*. 2020). Thus, the effect of the EB irradiation on the flow starting load was not affected by the type of the additives, water, or PF resin. The molding load was also decreased with increasing absorbed dose. The molding load is affected by the flow resistance in the wood disks and the friction between the disks and metal punches. During molding, the PF resin squeezed by the compression may intrude into the boundary between the disks and punches (Seki *et al*. 2016b). This may lead to the independence of the absorbed dose on the friction, as the quantity and quality of the treated wood may not be affected by the absorbed dose. The molding load decreased by the EB irradiation may be due to the decreased flow resistance of the disks.

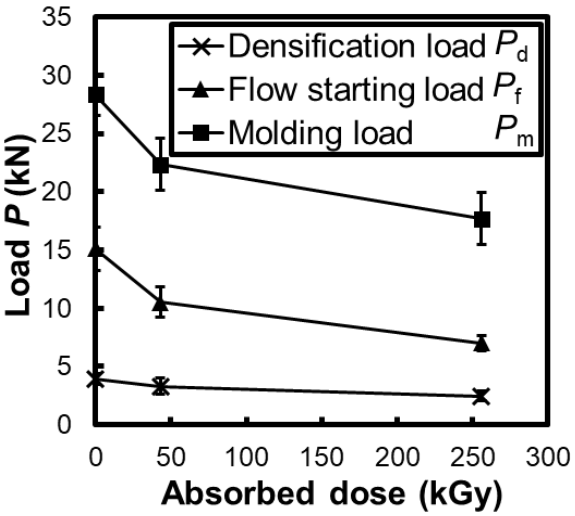

Fig. 7. Relation of densification, flow starting, and molding load to absorbed dose. Error bars represent standard deviations (n = 5).

Three-point bending test

Figure 8 shows the relation of MOE and MOR to the absorbed dose. MOE was slightly decreased with increasing the absorbed dose, and the decrease in the range of 43 to 256 kGy was smaller than the decrease in the range of 0 to 43 kGy. MOR was linearly decreased with increasing the absorbed dose. The density of the formed material from the disks for the dose of 0, 43, and 256 kGy was 1.35 ± 0.01 g/cm^3, 1.34 ± 0.01 g/cm^3, and 1.33 ± 0.01 g/cm^3, respectively. Thus, the density may not affect the decrease in both MOE and MOR. The decreasing rate for MOR was far larger than that for MOE. This may be because the defects caused by the EB-irradiation had the larger influence on the structure-sensitive MOR than the structure-insensitive MOE.

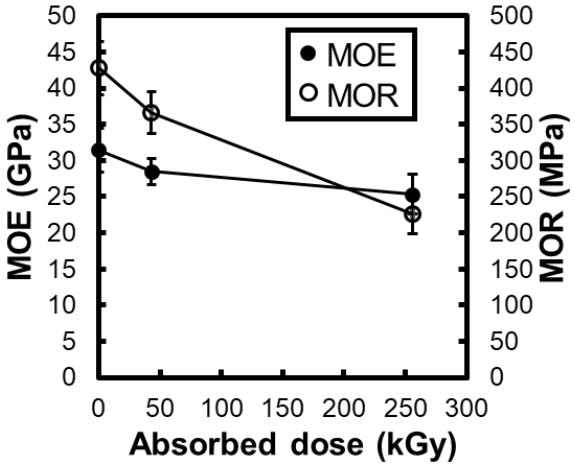

Fig. 8. Relations of MOE and MOR for formed material to absorbed dose. Error bars represent standard deviations (*n* = 5).

To understand the influence of the defects on MOR, the fracture morphology of the sample was observed for each dose. Figure 9 shows the light reflection image on the RL-surface (side surface) of the formed sample before and after the bending test. The image was obtained by digital microscope (VHX-5000, KEYENCE Co.). In the sample for 0 kGy (Fig. 9d), the simple crack across the L direction was continuous from the surface plane of the tension side to the neutral plane in the sample. The number of the cracks across the L direction tended to increase with increasing the absorbed dose (Figs. 9e and 9f). This was considered to be because the cellulose was damaged by the EB irradiation on the raw wood, leading to the decrease in the MOR (Fig. 8).

Relationship between molding load and mechanical properties

The relationship of MOE and MOR to the molding load is shown in Fig. 10. Both the MOE and MOR decreased with decreasing the molding load, and the decrease in MOR was larger than that in MOE. Furthermore, the decrease in MOR was accelerated by the decrease in the molding load. In the material utilization, the decrease in the mechanical properties was the fatal problem. For the EB irradiation on raw wood aimed at the lower molding load; therefore, it was necessary not to increase the absorbed dose too much.

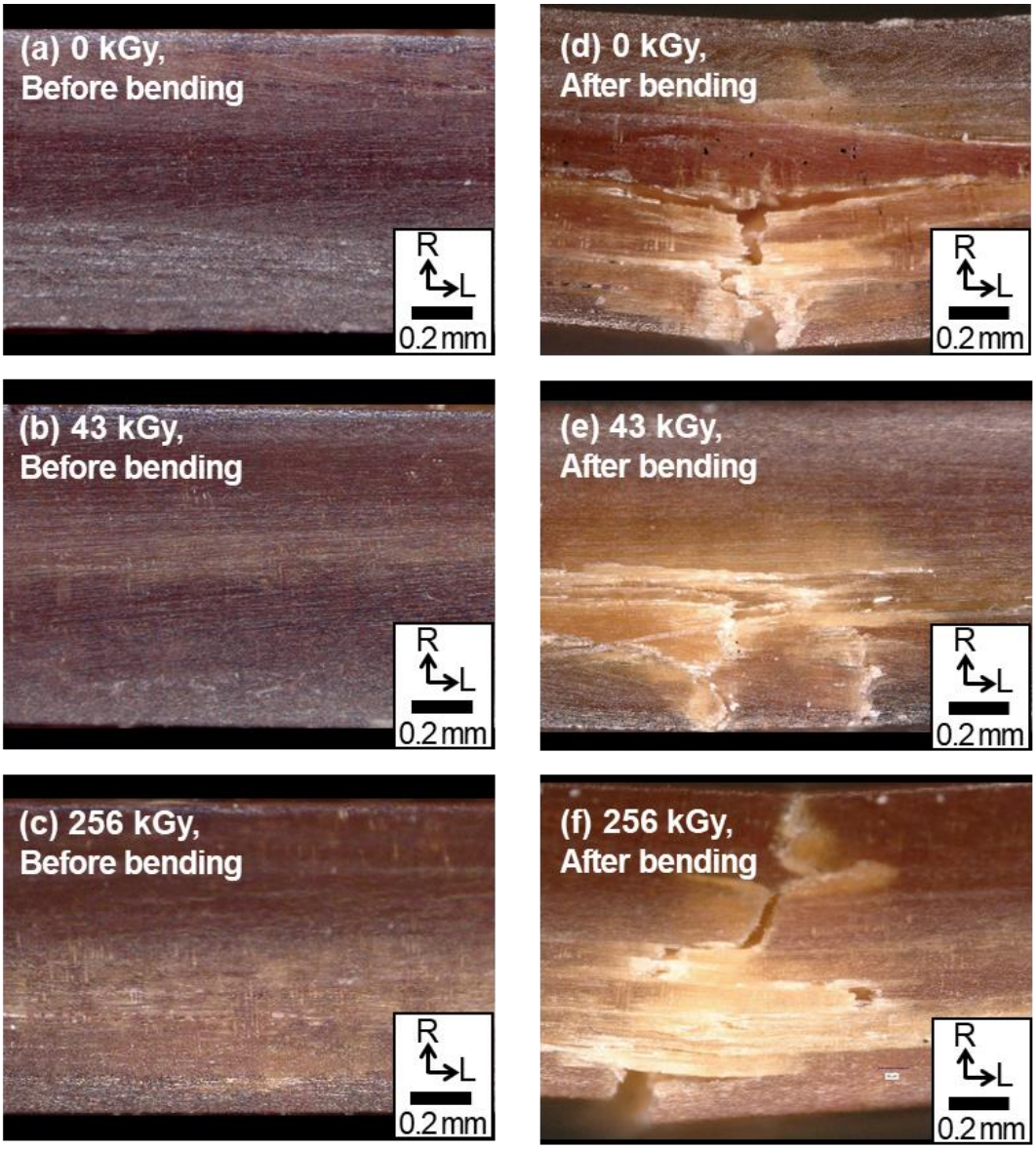

Fig. 9. RL-surface (side surface) of formed sample before and after three-point bending test

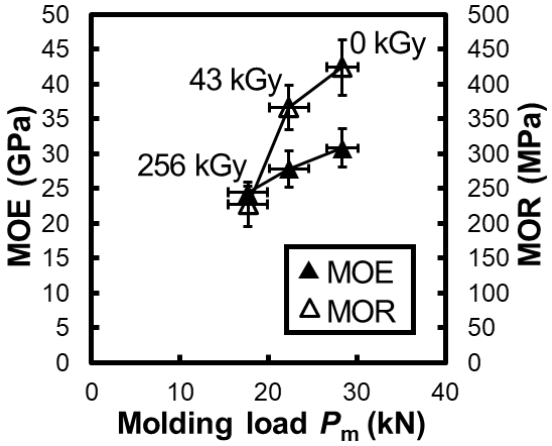

Fig. 10. Relations of MOE and MOR to molding load affected by EB irradiation on raw wood. Error bars represent standard deviations (n = 5).

CONCLUSIONS

1. The electron beam (EB)-irradiated wood board was treated with thermosetting resin and was subsequently molded into the material by adding pressure and heating in closed metal die. In the molding, both the flow starting load and the molding load were decreased with increasing the EB-absorbed dose.
2. Compression ratio at flow starting point in the molding was little affected by the absorbed dose.
3. Modulus of elasticity (MOE) and modulus of rupture (MOR) were measured for the molded material in the three-point bending test. With increasing the dose, MOR was decreased greatly while MOE was decreased slightly.
4. The EB irradiation on raw wood made it possible to mold the material in low load, though higher dose irradiation caused larger decreases in the mechanical properties.

REFERENCES CITED

Kashiwagi, M., and Hoshi, Y. (2012). "Electron beam processing system and its application," *SEI Technical Review* 75, 47-54. https://global-sei.com/technology/tr/bn75/pdf/75-09.pdf

Leskinen, T., Kelly, S. S., and Argyropoulos, D. S. (2017). "E-beam irradiation & steam explosion as biomass pretreatment, and the complex role of lignin in substrate recalcitrance," *Biomass and Bioenergy* 103, 21-28. DOI: 10.1016/j.biombioe.2017.05.008

Ma, X., Zheng, X., Zhang, M., Yang, X., Chen, L., Huang, L., and Cao, S. (2014). "Electron beam irradiation of bamboo chips: Degradation of cellulose and hemicelluloses," *Cellulose* 21(6), 3865-3870. DOI: 10.1007/s10570-014-0402-4

Mehnert, R. (1996). "Review of industrial applications of electron accelerators," *Nuclear Instruments and Methods in Physics Research Section B: Beam Interactions with Materials and Atoms* 113 (1-4), 81-87. DOI: 10.1016/0168-583X(95)01344-X

Miki, T., Seki, M., Sugimoto, H., Shigematsu I., and Kanayama, K. (2012). "Mechanical properties of wood plastic composites prepared by wood flow forming using low molecular phenol resin," in *Proc. of 11th Pacific Rim Bio-based Composites Symposium*, Shizuoka, Japan, pp.154-161.

Miki, T., Sugimoto, H., Shigematsu, I., and Kanayama, K. (2014). "Superplastic deformation of solid wood by slipping cells at sub-micrometre intercellular layers," *International Journal of Nanotechnology* 11(5–8), 509-519. DOI: 10.1504/IJNT.2014.060572

Miki, T., Nakaya, R., Seki, M., Tanaka, S., Sobue, N., Shigematsu, I., and Kanayama, K. (2015). "Flow behavior of wood treated with melamine formaldehyde resin under non-equilibrium thermal-compression," *Advanced Materials Research* 1119, 278-282. DOI: 10.4028/www.scientific.net/AMR.1119.278

Nakai, K., Sasuga T., and Sakamoto, O. (2009). "EB processing for industrial applications (in Japanese)," *Technical Report in Nissin Electric Co., Ltd.* 54(2), 9-21.

Saito, K., Horikawa, Y., Sugiyama, J., Watanabe, T., Kobayashi, Y., and Takabe, K. (2016). "Effect of thermochemical pretreatment on lignin alteration and cell wall

microstructural degradation in *Eucalyptus globulus*: comparison of acid, alkali, and water pretreatments," *Journal of Wood Science* 62, 276-284. DOI: 10.1007/s10086-016-1543-x

Schnabel, T., and Huber, H. (2014). "Improving the weathering on larch wood samples by electron beam irradiation (EBI)," *Holzforschung* 68 (6), 679-683. DOI: 10.1515/hf-2013-0181

Seki, M., Tanaka, S., Miki, T., Shigematsu, I., and Kanayama, K. (2016a). "Extrudability of solid wood by acetylation and in-situ polymerization of methyl methacrylate," *BioResources* 11(2), 4025-4036. DOI: 10.15376/biores.11.2.4025-4036

Seki, M., Miki, T., Tanaka, S., Shigematsu, I., and Kanayama, K. (2016b). "Friction characteristics between metal tool and wood impregnated with phenol formaldehyde (PF) resin during exposure to high pressure," *Journal of Wood Science* 62(3), 223-241. DOI: 10.1007/s10086-016-1551-x

Seki, M., Miki, T., Tanaka, S., Shigematsu, I., and Kanayama, K. (2017). "Repetitive flow forming of wood impregnated with thermoplastic binder," *International Journal of Material Forming* 10(3), 435-441. DOI: 10.1007/s12289-016-1291-x

Sugino, H., Tanaka, S., Kasamatsu, Y., Okubayashi, S., Seki, M., Miki, T., Umemura, K., and Kanayama, K. (2020). "Influence of electron-beam irradiation on plastic flow deformation of wood (in Japanese)," *Mokuzai Gakkaishi* 66(2), 59-66. DOI: 10.2488/jwrs.66.59

Tanaka, S. (2017). "Impregnation techniques for wood flow forming (in Japanese)," *Journal of the Adhesion Society of Japan* 53(3), 89-92. DOI: 10.11618/adhesion.53.89

Yamashita, O., Yokochi, H., Miki, T., and Kanayama, K. (2007). "Producing cups from wood by extrusion using flow phenomenon of bulk wood," *Transactions of the Japan Society of Mechanical Engineers A* 73(729), 29-34. DOI: 10.1299/kikaia.73.583

Article submitted: October 30, 2020; Peer review completed: November 27, 2020; Revised version received and accepted: April 12, 2021; Published: April 14, 2021.
DOI: 10.15376/biores.16.2.3895-3906